Microscopy and Microanalysis (2018), **24**, 38–48
doi:10.1017/S1431927618000065

Microscopy AND Microanalysis

Original Article

Early Effects of Ionizing Radiation on the Collagen Hierarchical Structure of Bladder and Rectum Visualized by Atomic Force Microscopy

Svetlana L. Kotova[1,2], Peter S. Timashev[3,4], Galina V. Belkova[1], Marina V. Kochueva[5], Ksenia V. Babak[6], Victoria A. Timofeeva[1], Elena B. Kiseleva[5], Olga O. Vasilieva[1], Anna V. Maslennikova[5] and Anna B. Solovieva[1]

[1]Department of Polymers and Composites, N.N.Semenov Institute of Chemical Physics, 4 Kosygin St., Moscow 119991, Russia, [2]Federal Research Clinical Center of the Federal Medico-Biological Agency of Russia, 28 Orekhovy Blvd., Moscow 115682, Russia, [3]Institute for Regenerative Medicine, I. M. Sechenov First Moscow State Medical University, 8 Trubetskaya st., Moscow 119991, Russia, [4]Research Center "Crystallography and Photonics", Institute of Photonic Technologies, 2 Pionerskaya st., Troitsk, Moscow 142190, Russia, [5]Nizhny Novgorod State Medical Academy, 10/1 Minin and Pozharsky Sq., Nizhny Novgorod 603005, Russia and [6]N.I.Lobachevsky Nizhny Novgorod State University, 23 Gagarin Ave., Nizhny Novgorod 603950, Russia

Abstract

Radiation therapy, widely used in the treatment of a variety of malignancies in the pelvic area, is associated with inevitable damage to the surrounding healthy tissues. We have applied atomic force microscopy (AFM) to track the early damaging effects of ionizing radiation on the collagen structures in the experimental animals' bladder and rectum. The first signs of the low-dose radiation (2 Gy) effect were detected by AFM as early as 1 week postirradiation. The observed changes were consistent with initial radiation destruction of the protein matrix. The alterations in the collagen fibers' packing 1 month postirradiation were indicative of the onset of fibrotic processes. The destructive effect of higher radiation doses was probed 1 day posttreatment. The severity of the radiation damage was proportional to the dose, from relatively minor changes in the collagen packing at 8 Gy to the growing collagen matrix destruction at higher doses and complete three-dimensional collagen network restructuring towards fibrotic-type architecture at the dose of 22 Gy. The AFM study appeared superior to the optical microscopy-based studies in its sensitivity to early radiation damage of tissues, providing valuable additional information on the onset and development of the collagen matrix destruction and remodeling.

Key words: Atomic force microscopy, collagen, radiation therapy, bladder, rectum

(Received 9 March 2017; revised 14 December 2017; accepted 12 January 2018)

Introduction

In spite of the developing techniques of conformal radiation therapy, its adverse effects on the normal tissues within the irradiated volume during the treatment of malignant neoplasms still present an important problem of the modern clinical oncology (National Institutes of Health, 2010). The effects are of particular importance for patients with a long-life expectancy, for whom the quality of life plays a no less crucial role than the cure from the oncological disease does.

The main cause of the late complications, arising more than 3 months after the completion of the irradiation course, is radiation-induced fibrosis, which appears as a result of neo-collagenesis in the radiation-damaged tissues (Trott et al., 2012).

One of the key mechanisms for the development of normal tissues' radiation damage is degradation and subsequent remodeling of the connective tissue matrix. The collagen synthesis activation in irradiated tissues leads to the radiation-induced fibrosis, which is accompanied by the corresponding organs' dysfunction, that is typical of the second grade of radiation changes. The main manifestation of complications of the third and fourth grades is the degradation of extracellular matrix (ECM) components, which leads to the subsequent appearance of necrosis, bleeding, and fistula. (Trott et al., 2012). The molecular and genetic mechanisms of the development of radiation damage have been studied in detail (Denham & Hauer-Jensen, 2002; Yarnold & Brotons, 2010). However, only scarce information is available on the processes of damage and subsequent remodeling of the ECM which occur early (in <3 months term) after the action of ionizing radiation. Studies on the structural alterations of collagen after irradiation in lower doses revealed changes in its physico-chemical properties, indicating formation of a more "rigid" biopolymer structure, violation of the parallel packing, and reduction of the collagen fibers' thickness (Tzaphlidou et al., 1997) and increase in the malonic dialdehyde concentration (Balli et al., 2009). The most recent laser scanning microscopy and differential scanning calorimetry (DSC) studies using a model medium have demonstrated that the basic mechanism of collagen radiation damage at the molecular and fibrillar (i.e. nano structural) level involves formation of tears and cross-links (proven by DSC), whereas at the level of bundles it involves their

Author for correspondence: Svetlana L. Kotova, E-mail: slkotova@mail.ru

Cite this article: Kotova SL, Timashev PS, Belkova GV, Kochueva MV, Babak KV, Timofeeva VA, Kiseleva EB, Vasilieva OO, Maslennikova AV and Solovieva AB (2018) Early Effects of Ionizing Radiation on the Collagen Hierarchical Structure of Bladder and Rectum Visualized by Atomic Force Microscopy. *Microsc Microanal* **24**(1): 38–48. doi: 10.1017/S1431927618000065

dissection with the following "healing" of the gaps (demonstrated by laser scanning microscopy). No changes in the collagen fibers have been found (Maslennikova et al., 2015). These findings are in accord with the directly visualized radiation damage of collagen fibrils in the electron microscope, in particular, the progressive destruction of fibrils with increasing dose (Grant et al., 1973). The recent multiphoton microscopy study of the bladder ECM (Kuznetsov et al., 2016) has shown that, following the ionizing radiation treatment, a reduction of the second harmonic generation signal is observed for the irradiated specimens, which indicates a disorder of the anisotropic pseudo-crystalline packing of collagen.

In the last two decades, atomic force microscopy (AFM) has found a plethora of biomedical applications due to a growing interest towards the nanoscale changes taking place in the living tissue (see, e.g., a recent review by Maver et al., 2016). In particular, AFM has been extensively used in the studies of the ECM complex architecture, which is mainly constructed of a fibrous collagen network both at the nanoscale and microscale. These studies have shown that the collagen matrix morphology at different scales, as well as its elastic properties, are not only crucial for the functioning of various types of connective tissue, but may also reflect pathological processes occurring in the connective tissue (Sivasankar & Ivanisevic, 2007; Stolz et al., 2009; Graham et al., 2010; Wallace, 2012; Wen et al., 2012; Zhu & Fang, 2012; Kwok et al., 2014; Thomasy et al., 2014; Kim et al., 2016; Jorba et al., 2017).

In our previous studies (Kotova et al., 2015; Timashev et al., 2016), we have developed an AFM-based approach to tracking pathological alterations of the collagen hierarchical structure in ECM of various tissues, which may be used as a complimentary technique to the traditional histological clinical assessment. In this study, we apply the same approach to probe early negative effects of ionizing radiation on the healthy tissue of pelvic organs (bladder and rectum). As these effects are hardly (if at all) detectable by traditional biomedical optical microscopy methods, we expect that AFM modalities might provide a new insight into the problem of early damage in the collagen-containing tissues following radiation therapy.

Materials and methods

Preparation of Samples

The studies were performed on white outbred rats (20 animals in total) homed in standard vivarium conditions in accordance with the requirements of the legal acts regulating research on the safety and efficacy of pharmaceutical substances in the Russian Federation (The Order No. 267 of the Ministry of Healthcare of the Russian Federation of June 06, 2003) and the international laws on the legal and ethical norms of animal studies. Before irradiation, the experimental animals were anesthetized (Zoletil 50 mg/kg of weight). Then the animals were fixed on a special plate, and irradiation was performed by a local pelvic field that included bladder and rectum by a single dose of 2 Gy up to total doses of 2 Gy (one fraction, four animals), 8 Gy (four fractions, four animals), 10 Gy (five fractions, four animals), and 22 Gy (11 fractions, four animals). The exposure time was calculated in accordance with the size of the irradiation field, the depth, and the single dose. Irradiation was carried out in vivo using the Co60 unit "Terabalt" (UJP Praha-Zbraslav, Czech Republic, beam energy 1.25 MeV).

For the low-dose irradiation of 2 Gy, the animals were sacrificed with ether narcosis in 1 day, 1 week, and 1 month postirradiation, and the bladder, rectum, and a fragment of skin within the irradiation projection were harvested. For the higher doses, the tissues' harvesting was performed 1 day postirradiation. Four intact (nonirradiated) rats were used as a control group. The harvested tissues were dissected, the samples for the histology study were fixed for 24 h in a 10% neutral formalin solution. Then, the samples were embedded in paraffin wax ("Histomix-extra"; Biovitrum, St. Petersburg, Russia) with subsequent paraffin block mounting. Slices, 0.3 μm and 10 μm thick, were prepared with a Leica 450RM rotary microtome (Leica Microsystems, Wetzlar, Germany). The 0.3 μm-thick sections were stained with van Gieson's picrofuchsin. The 10 μm-thick sections from the same blocks were thoroughly deparaffinized and left unstained for the AFM study. The bladder, rectum, and skin of intact animals were used as control samples.

The protocol of preparation was reproduced in detail for all the samples, to eliminate the effects of samples' processing (e.g., Choy et al., 2005, Dorph-Petersen et al., 2001).

AFM Imaging Study

AFM images of the fixed tissue slices on glass slides were acquired with a Solver P47 AFM instrument (NT-MDT, Zelenograd, Russia), in the semi-contact mode, using a precision scanner ($14 \times 14 \times 2\,\mu$m, Solver, NT-MDT) and silicon TESP probes (Bruker, Santa Barbara, CA, USA). General-view $14 \times 14\,\mu$m images and detailed $6 \times 6\,\mu$m and $3 \times 3\,\mu$m topography and phase images were obtained at a scan rate of 1 Hz and a 512×512 pixels resolution.

The regions of interest (ROI) for scanning were selected in accordance with the histological assignments for the same sample, based on the view of a sample in the built-in optical microscope of the AFM instrument setup (Fig. 1). The submucosal layer rich with collagen fibers was studied for all the samples. At least ten images from different regions of each section were acquired. For visualization, AFM images underwent standard processing (flattening and cleaning) with the image processing software Nova (NT-MDT, version 1.0.26.1443). Raw images without any processing were used in the flicker-noise spectroscopy (FNS) computations.

FNS for AFM Images

For the quantitative assessment of the changes in the ECM morphology visualized by AFM imaging, we applied a FNS

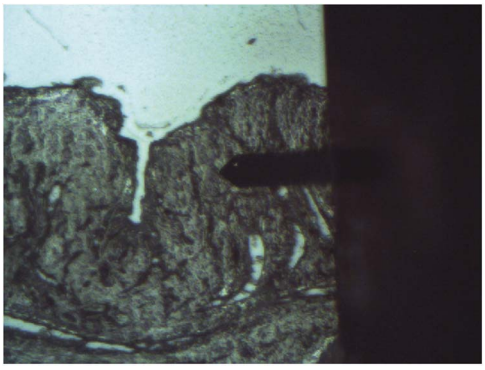

Figure 1. Optical microscopy image of a rat bladder section with the atomic force microscopy tip in contact.

https://doi.org/10.1017/S1431927618000065 Published online by Cambridge University Press

parameterization technique (Mirsaidov et al., 2011). In the FNS approach, the roughness profiles $h(x)$ in every y-line in an AFM image is considered as a series of chaotic signals (dynamic variables), and the FNS technique seeks correlations in these series. The derived surface FNS nanometrology parameters are related to the autocorrelation function for every profile. The FNS power spectra allow selection of different ranges of spatial frequencies in the $h(x,y)$ profiles. The low-frequency (resonant) range (which mostly reflects major bends of the surface originating from the macromanipulations such as sample positioning) is disregarded. The high-frequency range is described in the terms of two basic types of sharp irregularities. The first type—"jumps"—represent relatively moderate-height steps against the low-frequency baseline. The second type—"spikes"—are single intense bursts of the signal. Each of these two types of irregularities is ascribed a corresponding FNS parameter: a "stepwiseness factor" σ (nm) for the jump-like irregularities and a "spikiness factor" $S(L_0^{-1})$ (nm$^2\mu$m) for the spike-like irregularities (where L_0 is the length of correlation for the nanoscale high-frequency irregularities in the profile). There exist also other FNS parameters, which are of a relatively minor importance for AFM images. The entire FNS procedure, including the derivation and calculation of the "stepwiseness factor" σ and the "spikiness factor" $S(L_0^{-1})$ is presented in (Mirsaidov et al., 2011).

We used the two above FNS parameters—"stepwiseness factor" σ and the "spikiness factor" $S(L_0^{-1})$—to quantitatively characterize the visualized surface morphology of the ECM before and after irradiation. The rationale behind our choice of the FNS parameterization instead of a standard metrological roughness (ISO 4287) lies in the fact that the surface of tissue slices has considerable height heterogeneity and, besides, the features determined by the inner structure of a sample, reflect also the entire sample history from pretreatment to drying to microtome sectioning. For such surfaces, the standard metrological parameters are generally not informative. In contrast, the FNS parameterization, via a careful analysis of frequencies in the power spectra, along with the visual assessment of the corresponding images, allows elimination of the systematic artifacts and extraction of the sample's intrinsic structure parameters.

The FNS computations were performed according to the algorithm described in Mirsaidov et al. (2011) using custom-coded software.

Histological Study

The histological study was performed as a standard technique for assessment of the collagen structures' damage and also for the correct assignment of the ROI in the AFM study. We used a standard van Gieson's staining protocol to distinguish between collagen fibers and other components of the tissue. Stained sections, 0.3 μm thick, were studied with a Leica DM2500 microscope (Leica Microsystems) equipped with a DFC 245C digital camera. The digital micrographs were obtained at an original magnification of 20× and presented as 370 × 370 μm images.

Results

Early Effects of Low-Dose Irradiation on the Bladder and Rectum: Effect of the Time Elapsed After the Radiation Treatment

The AFM studies of the bladder and rectum (submucosal region) were conducted 1 day, 1 week and 1 month following the irradiation of the animals from the experimental group with a low-radiation dose of 2 Gy. The tissues harvested from the intact rats (control group) were studied as a reference.

The Low-Dose Radiation Effects on the Bladder

Collagen fibers of the normal bladder ECM form a characteristic wavy pattern, in which the bundles of fibers are densely interlaced (Fig. 2, 1A), similar to the "basket-weave" packing of collagen fibers in ECM of other connective tissue, such as skin or arterial walls (Graham et al., 2010; Timashev et al., 2016). The collagen fibrils inside the fibers are partially covered with an unstructured proteinaceous material and partially are naked (Fig. 2, 1B and 1C), the packing pattern of fibrils at the nanoscale (visible in the naked regions) generally resembles that of collagen fibers observed at the microscale.

One day postirradiation, no visible changes were observed both in the collagen fibers and collagen fibrils packing, as compared with the intact tissue ECM. 1 week after the radiation treatment, we detected an essential decrease in the fraction of uncovered regions and appearance of regions entirely covered with a thick layer of an unstructured material (Fig. 2, 2B and 2C), so that even the contours of collagen fibrils were no longer distinguishable. These changes still did not affect the packing of collagen fibers and their bundles (Fig. 2, 2A). However, in a month after the irradiation, drastic changes occurred at all the levels of collagen organization in the bladder ECM. In contrast to the intact tissue, 1 month postirradiation collagen fibers tended to conglomerate into thick locally oriented bundles (Fig. 2, 3A) of a significant width. The high-resolution AFM images revealed densely packed fibrils with a predominantly parallel packing inside such fibers (Fig. 2, 3B and 3C). In some regions, collagen fibrils retained their initial three-dimensional (3D) network, in other regions spherical proteinaceous particles covered the fibrils. No changes in the D-period of collagen and in the thickness of collagen fibrils were detected for any samples at the different time points after the irradiation.

The Low-Dose Radiation Effects on the Rectum

The overview AFM images (Fig. 3, 1A) visualize a 3D network of collagen fibers in the submucosal region of the rectum. In the intact tissue, this structure has a mesh-like appearance, with the 1–2 μm average thickness of fibers. These fibers are formed by a finely interlaced 3D network of thin collagen fibrils (Fig. 3, 1B and 1C). Similar to the case of the bladder, the fibrils are partly naked, partly covered with spherical proteinaceous particles. Besides the collagen network, thick fibers without an inner fibrillar structure are observed, presumably elastin fibers. One day after the irradiation, no visible ECM changes were found both at the level of collagen fibers and fibrils.

In the samples harvested 1 week after the irradiation, the 3D structure of the intact tissue was generally preserved, however, the regions started to appear in which collagen fibers were essentially thicker and denser (Fig. 3, 2A). The packing of collagen fibrils remained mostly unchanged (Fig. 3, 2B and 2C). One month posttreatment, we observed rather notable morphological alterations for all the collagen structures. The collagen fibers in the rectum samples 1 month postirradiation formed dense oriented structures of a significant thickness (3–7 μm), as opposed to the initial meshwork of fibers. Thus, the collagen structures in both organs—bladder and rectum—underwent similar alterations in a 1-month period. Inside the thick oriented collagen fibers,

https://doi.org/10.1017/S1431927618000065 Published online by Cambridge University Press

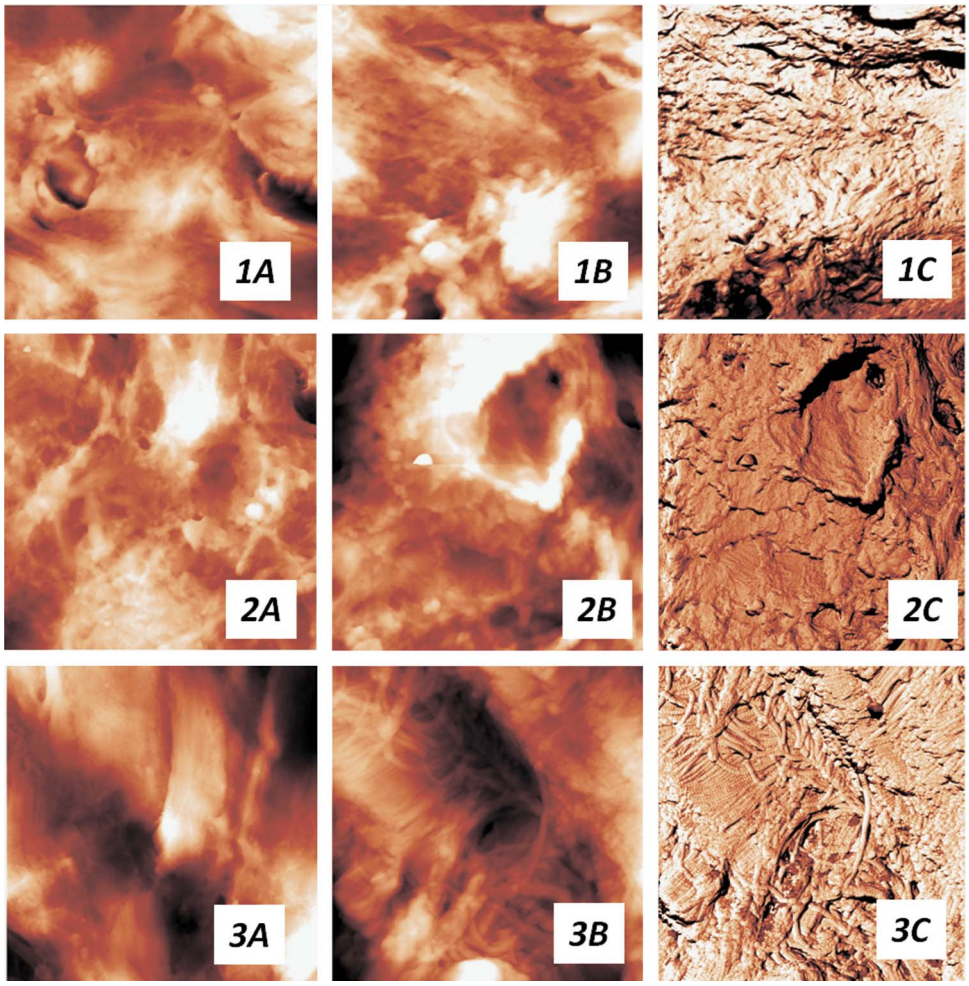

Figure 2. The bladder extracellular matrix changes with the time elapsed from the low-dose (2 Gy) treatment. **a**: Topography images, the scan size is 14 × 14 μm, (**b**) topography and (**c**) corresponding phase images, the scan size is 6 × 6 μm. 1, control group; 2, 1 week postirradiation; 3, 1 month postirradiation.

high-resolution imaging reveals a very dense fine-meshed network of collagen fibrils (partially covered with a continuous layer of an unstructured material). The characteristic D-period of collagen, as well as the average thickness of fibrils, did not change after the irradiation at any studied time point.

FNS Characterization of the Low-Dose Radiation Effects on the Bladder and Rectum

To quantify the changes in the collagenous network morphology caused by the low-dose radiation, we applied the FNS technique for parameterizing the 3D images obtained by AFM. Figure 4 displays the results of the FNS image analysis for the bladder and rectum ECM at different time points. For the bladder, both FNS parameters ("stepwiseness factor" σ and the "spikiness factor" S (L_0^{-1})) experienced a slight decrease 1 day postirradiation, after which they tended to return to the initial (or slightly above initial) values observed for the intact tissue. For the rectum, the FNS parameters, as well, slightly decreased 1 day postirradiation, but they remained slightly decreased at all the following time points, as compared with the initial values. In general, the FNS parameterization did not reveal significant differences between the studied samples which could be ascribed to the observed visual distinctions.

Histological Assessment of the Low-Dose Radiation Effects on the Bladder and Rectum

The histological study showed that the basic localizations of fibrous (collagen and elastin) structures in the rat bladder were the urothelial basal membrane, lamina propria, submucosa, walls of the blood vessels and the stromal backbone of the muscular layer (Fig. 5, b1, b3). The collagen/elastin ratio differed between the layers, with elastin fibers dominating in the basal membrane and collagen fibers dominating in the lamina propria and the submucosal region. No differences were found in the ECM of the bladder harvested 1 day postirradiation at the dose of 2 Gy, as compared with the control tissue ECM. One week postirradiation, slight alterations in the contour of the urothelial basal membrane were found, whereas the submucosa showed no difference with the intact tissue. One month after the irradiation, no signs of the collagen/elastin elements' alteration were detected in any regions of the bladder wall.

According to the histological study, the intact rectum wall has a layered structure with the clearly visible epithelium, basal membrane, lamina propria and the submucosal region. The basal membrane has an ordered fibrous structure with predominating elastin fibers. The lamina propria and submucosa consist mainly of a network of collagen fibers with a minor addition of elastin and muscular fibers (Fig. 5, R1, R3). In general, the basic

https://doi.org/10.1017/S1431927618000065 Published online by Cambridge University Press

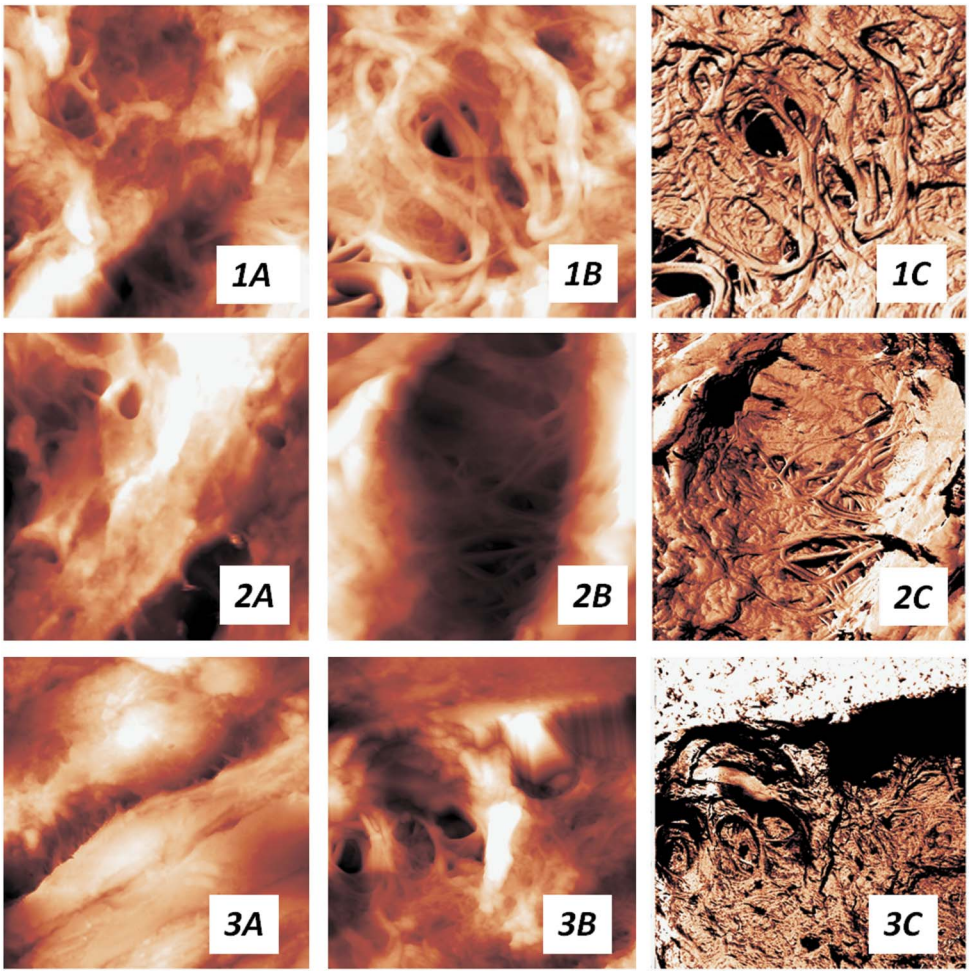

Figure 3. The rectum extracellular matrix changes with the time elapsed from the low-dose (2 Gy) treatment. **a**: Topography images, the scan size is 14 × 14 μm, (**b**) topography and (**c**) corresponding phase images, the scan size is 6 × 6 μm. 1, control group; 2, 1 week postirradiation; 3, 1 month postirradiation.

localizations of collagen and elastin fibers in the intact rat rectum are basal membrane, lamina propria, submucosa, walls of blood vessels and the stromal backbone of the muscular layer. After the low-dose irradiation of 2 Gy, no visible changes in the rectum connective tissue were revealed, independently of the time elapsed after the treatment.

Early Manifestations of the Radiation Damage of Pelvic Organs: Effects of the Radiation Dose

The earliest changes of the bladder and rectum connective tissue were captured with AFM imaging 1 day after the irradiation in the increasing doses of 2, 8, 10, 12, and 22 Gy. The intact tissues from the control group were used as a reference.

The Radiation Dose Effects on the Pelvic Organs' ECM Microstructure: Packing of Collagen Fibers

As was mentioned above, the low-dose radiation (2 Gy) treatment had no immediate effect on the ECM of the bladder and rectum. However, the higher doses of radiation resulted in visible changes in both organs, from relatively minor alterations of the collagen fiber packing at the 8 Gy dose to a very pronounced effect at the 22 Gy dose. As seen from Fig. 6, B2, 1 day after the irradiation at the dose of 8 Gy, the initial rather dense and isotropic 3D network of collagen fibers in the bladder becomes looser, and thick (several microns across) fibers appear against the finely meshed network background. After the 12 Gy treatment, the loose network of thick fibers prevails over the initial pattern. 1 day postirradiation in the dose of 22 Gy, the loose thick collagen fibers are mostly covered with a thick layer of an unstructured material (Fig. 6, B3). A similar trend was observed for the rectum samples harvested 1 day after the irradiation in different doses, but the collagen disorganization appeared even more pronounced than that in the bladder ECM (Fig. 6, R1, R3). At the 8 Gy dose (Fig. 6, R2), the loosening of the collagen fibers 3D network (compared with the intact ECM) was notable, at the 12 Gy point the thick disorganized fibers were covered with a continuous layer of globules. 1 day after the 22 Gy radiation treatment (Fig. 6, R3), the entire pattern of the collagen fibers packing was dramatically altered, as compared with the control tissue: collagen fibers formed wide oriented bundles, coated with thick layers of globules or solid unstructured material.

As both organs (bladder and rectum) experienced similar alterations of the collagen structures under the same irradiation regimes, we additionally studied the abdominal skin samples harvested from the irradiated spots, to compare the observed changes with those for a different type of connective tissue (Fig. 6, S1–S3). The AFM imaging study showed drastic effects of radiation on the skin ECM already at a rather low dose of 8 Gy—loosening and thickening of collagen fibers and production of a great amount of nonfibrous components of the ECM covering the

https://doi.org/10.1017/S1431927618000065 Published online by Cambridge University Press

fibers (Fig. 6, S2). These effects advanced with the dose (Fig. 6, S3), completely destroying the initial characteristic basket-weave pattern of the skin in this area (Kotova et al., 2015).

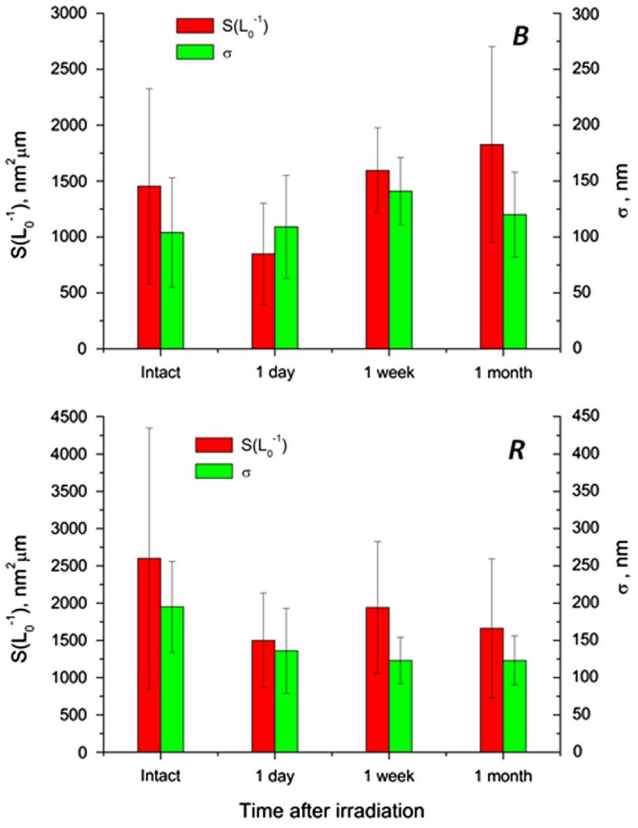

Figure 4. Flicker-noise spectroscopy parameterization of the atomic force microscopy (AFM) images of the pelvic organs extracellular matrix, at different time points after the low-dose (2 Gy) irradiation. The sizes of the processed AFM images are 6 × 6 μm. B, bladder; R, rectum.

The Radiation Dose Effects on the Pelvic Organs' ECM Nanostructure: Packing of Collagen Fibrils

The high-resolution AFM imaging revealed that the radiation-induced changes in the pelvic organs occurred not only in the packing of collagen fibers, but also in the organization of fibrils inside the fibers.

The low dose of 2 Gy had no effect on the packing of collagen fibrils the next day after the treatment for all the tissues under study (Figs. 2, 3). With the radiation dose increase, the bladder collagen fibrils tended to thicken (Fig. 7, B2) and finally lose their local tight quasi-parallel arrangement, forming a rather disordered structure (Fig. 7, B3), partially covered with a non-fibrous ECM material. For the rectum, the loss of tight fibrils packing and a thick coating with unstructured proteinaceous substance was observed already at 8 Gy (Fig. 7, R2). For the higher doses, the AFM imaging demonstrated complete coverage of collagen fibrils with a thick continuous layer of this substance (Fig. 7, R3).

The collagen fibrils in the skin ECM also underwent changes with the increase of radiation dose. The initial network of fibrils in the skin has a basket-weave appearance with chaotic interlacing of fibrils (Graham et al, 2010; Kotova et al., 2015). After the radiation treatment (Fig. 7, S1–S3), collagen fibrils in the skin acquired a tendency to quasi-parallel packing (unlike the bladder and rectum ECM fibrils) with an increase in the fibrils' thickness (similar to the bladder fibrils). The growth in the amount of nonfibrous ECM material covering the fibrils with the radiation dose appeared characteristic for all the irradiated tissues.

No changes in the characteristic D-period of collagen were found in this study.

FNS Characterization of the Dose Radiation Effects on the ECM of the Pelvic Organs

The changes in the collagen structures of the pelvic tissues irradiated in different doses, visualized with AFM imaging, were summarized in a numerical form using the FNS parameterization.

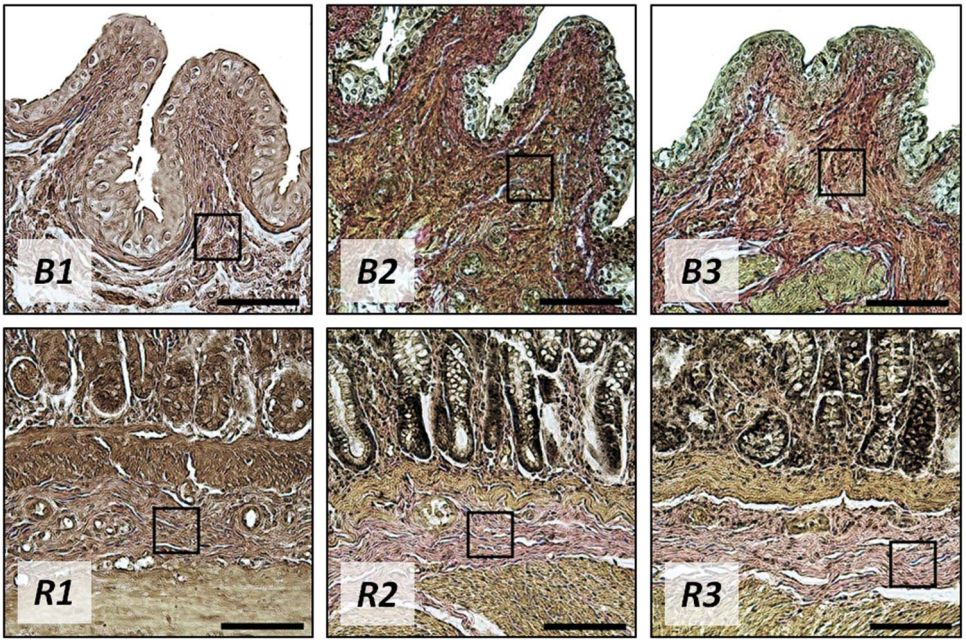

Figure 5. The bladder (B) and rectum (R) cross-sections 1 day (1), 1 week (2), and 1 month (3) after the 2 Gy treatment, histological study. Van Gieson's stain, original magnification: 20×. Black squares mark the regions of interest for the atomic force microscopy study. Bar = 100 μm.

https://doi.org/10.1017/S1431927618000065 Published online by Cambridge University Press

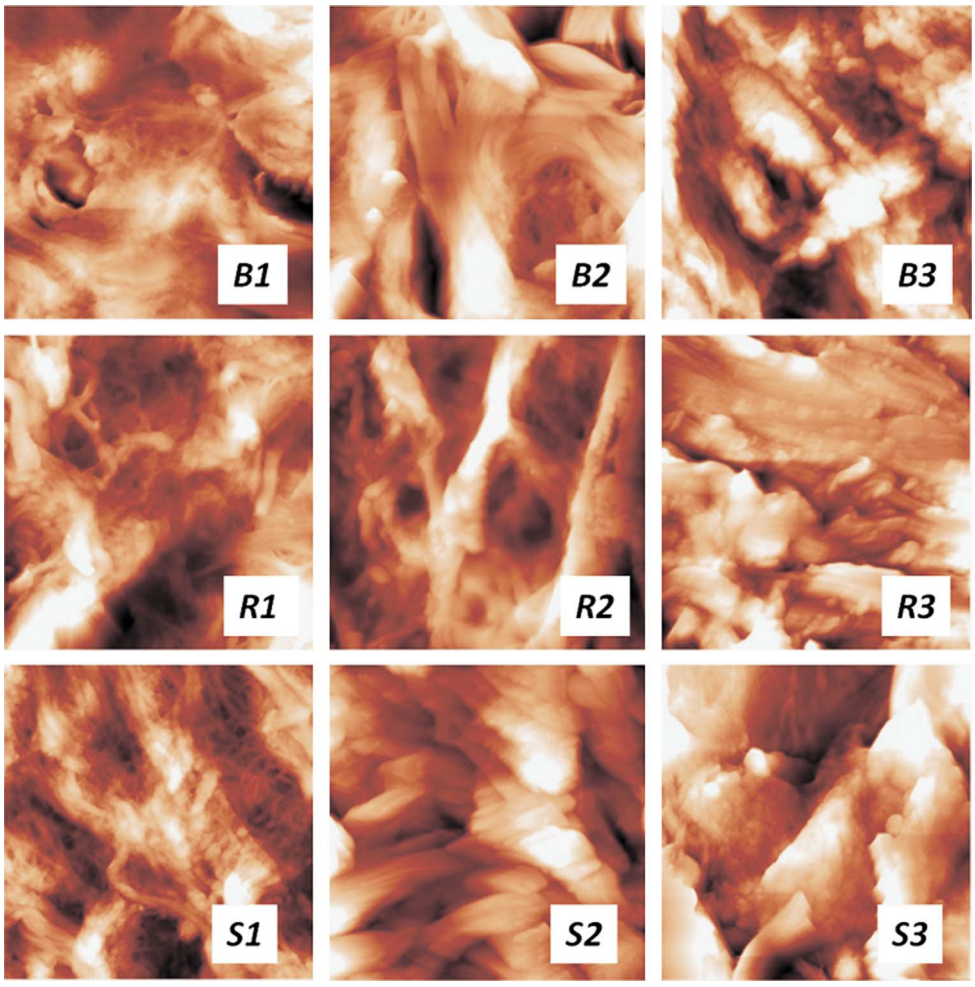

Figure 6. The changes of collagen fibers' packing with the radiation dosage for pelvic tissues. Control samples (1) and samples 1 day after the irradiation in the dosage of 8 Gy (2) and 22 Gy (3). B, bladder; R, rectum; S, skin. The scan sizes are $14 \times 14\,\mu$m.

The results of the FNS image analysis for the bladder, rectum, and skin ECM 1 day postirradiation in different doses are presented in Fig. 8. In contrast to the absence of significant changes of the FNS parameters related to the visualized differences in the bladder and rectum morphology at different time elapsed after the treatment (1.3), the dose dependence of the FNS parameters not only was quite pronounced, but also showed a striking similarity between the bladder, rectum, and skin. The FNS parameters ("stepwiseness factor" σ and the "spikiness factor" $S(L_0^{-1})$) demonstrated almost the same character of dependencies on the radiation dose. In general, the increase of the radiation dose resulted in the increase of the FNS parameters, which, in terms of the FNS theory (Mirsaidov et al., 2011) corresponds to the growth of disorder in the system and thus well correlates with the visually observed morphological changes in the collagen structures. At the highest dose of 22 Gy, the values of the FNS parameters dropped, which is obviously related to the smoothening of the surface due to the thick coating of collagen fibers with an unstructured material.

Histological Assessment of the Radiation Dose Effects on the Bladder and Rectum

The radiation of the bladder, rectum, and skin in the higher doses resulted in the interstitial edema of the submucosal region, which, in Van Gieson-stained sections, presented itself as insignificant thickening of collagen fibers and increase in the distances between the structural elements of the ECM in all the organs under study (Fig. 9). The degree of these alterations grew proportionally to the radiation dose.

Discussion

The radiation damage of bladder and rectum is of primary concern in the radiotherapy of pelvic tumors, as these organs are located within the treatment field volume of a large number of malignancies, such as tumors of uterus and cervix, prostate, etc. The connective tissue of these organs, including the submucosa, which provides easy displacement and expansion of the mucosa, undergo damage and the subsequent remodeling after irradiation. According to the modern view of the radiation damage mechanisms (Atkinson, 2013), during the acute phase of the ECM damage, both the direct destruction of collagen molecules by highly reactive species appearing along the radiation track (Reisz et al., 2014) and over-expression of proteolytic enzymes towards the ECM components are related to the initial ECM lysis after irradiation. This initial activation of the ECM destruction is believed to give rise to the following over-production of the ECM components which leads to postradiation fibrosis. The later stages of the ECM postirradiation alterations, which appear days to months after the treatment, include activation of fibroblasts at the irradiated site and hyperproduction of collagen, as well as

https://doi.org/10.1017/S1431927618000065 Published online by Cambridge University Press

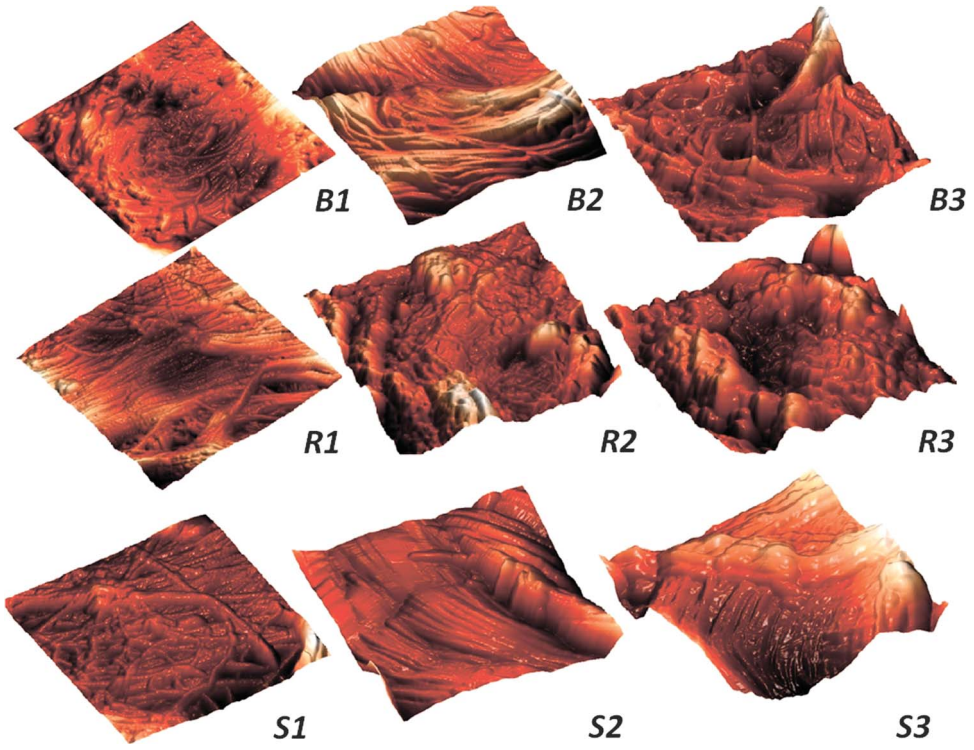

Figure 7. Reorganization of collagen fibrils with the radiation dosage increase for pelvic tissues. Control samples (1) and samples 1 day after the irradiation in the dosage of 8 Gy (2) and 22 Gy (3). B, bladder; R, rectum; S, skin. The scan sizes are $3 \times 3\,\mu$m, three-dimensional images.

fibronectin and laminin, which may or may not return to the normal levels.

Our AFM study suggests that collagen fibers in the submucosa of intact rat bladder are packed in densely interlaced bundles forming a wavy pattern. The same pattern is maintained at the nanoscale in the packing of collagen fibrils. The microstructure of the collagen backbone of the rectal submucosa is formed by a 3D meshwork of fibers, which consist of a smaller-scale finely interlaced network of thin collagen fibrils.

The low-dose (2 Gy) radiation treatment had no immediate effect on the hierarchical collagen structures in the bladder and rectum, as was shown for the tissue samples harvested 1 day postirradiation. 1 week after the treatment, the first changes at the level of fibrils were detected in the bladder, in which we observed a visible decrease in the fraction of naked collagen fibrils and appearance of regions entirely covered with a thick layer of unstructured material. The rectum collagen fibrils also underwent changes, but the character of these changes was different from the bladder—in the rectum, we observed appearance of regions with essentially thicker and denser fibrils. The packing of collagen fibers remained intact in both tissues at this time point. The revealed effects may reflect the initial matrix protein destruction processes which take place early in the course of radiation damage development, as well as the processes of inflammation (Atkinson, 2013). Both types of postradiation changes have been observed earlier for other types of connective tissue. In articular cartilage (Lindburg et al., 2013), a disruption in the binding between the collagen structures and glycosaminoglycans (GAG) was found after a radiation treatment with the 2 Gy dose, leading to the GAG release. In the case of irradiated bladder, the released nonfibrous components of ECM, including GAG, may form the continuous layer of unstructured material covering the collagen fibrils. Thickening of collagen fibrils after a 5 Gy treatment was detected in the skin ECM (Leontiou et al., 1993) and assigned to the disrupted collagen biosynthesis and binding.

Drastic alterations of the ECM structure were observed 1 month after the low-dose (2 Gy) irradiation. In the bladder, AFM imaging visualized thick bundles of collagen fibers with a pronounced unidirectional orientation. The fibrils inside the fibers were tightly packed in a quasi-parallel manner. Similar thick cords of collagen fibers were found in the rectal samples 1 month postirradiation. These findings may indicate the onset of postradiation fibrotic changes in both the bladder and rectum samples (Atkinson, 2013).

In the study of the low-radiation effects, the FNS procedure did not provide any additional information, as it showed no clear correlations between the time elapsed after the treatment and the FNS parameters extracted from the AFM images. It should be noted that, while FNS power spectra do demonstrate the intrinsic periodicity of collagenous structures (D-period), in general, FNS parameters have no direct reference to the measurable characteristics of ECM, such as the collagen content or fibrils' dimensions. However, correlations in the chaotic surface profiles (revealed by the FNS analysis) frequently appear rather sensitive to the structure ordering/disordering due to various processes (Kotova et al., 2015; Timashev et al., 2016), and thus the FNS parameters derived from such correlations may be used as markers for a comparative analysis of the ECM structure. The absence of such sensitivity in the case of the studied time dependencies may be related to the interplay of different processes which affect the order of the surface structure in the opposite manner: disordering of the collagen structure due to the radiation damage to the ECM versus the surface smoothening with the unstructured nonfibrous material and ordering due to the beginning fibrotic changes.

https://doi.org/10.1017/S1431927618000065 Published online by Cambridge University Press

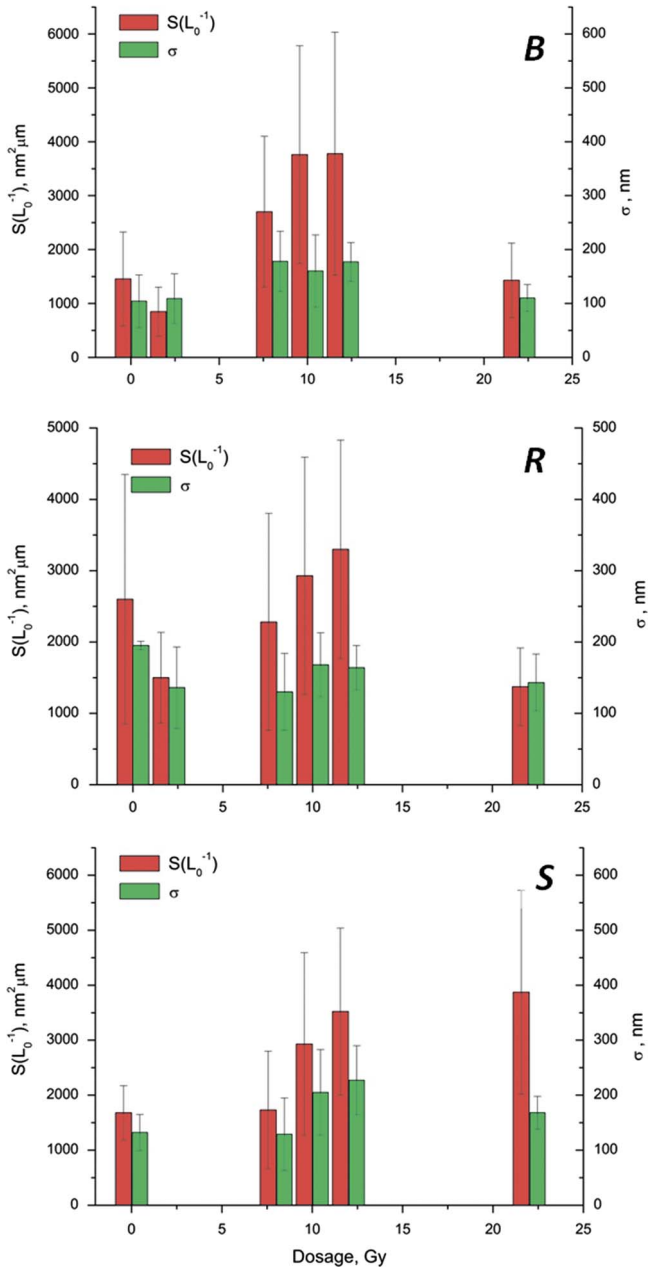

Figure 8. Flicker-noise spectroscopy parameterization of the atomic force microscopy (AFM) images of the pelvic organs extracellular matrix, different radiation doses. The sizes of the processed AFM images are 6 × 6 μm. B, bladder; R, rectum; S, skin.

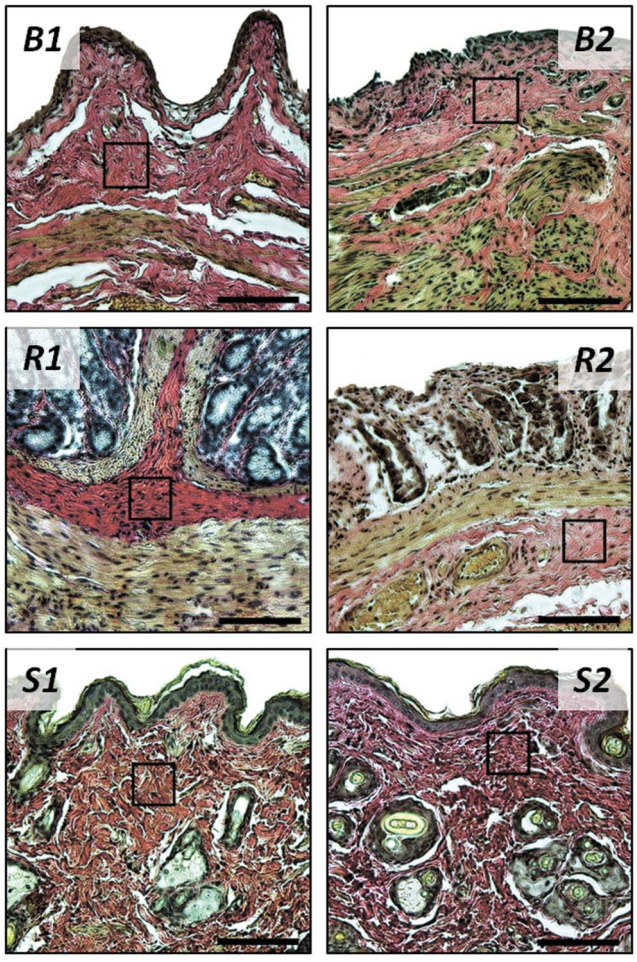

Figure 9. The bladder (B), rectum (R), and skin (S) cross-sections, control samples (1) and samples 1 day after the 22 Gy treatment (2), histological study. Van Gieson's stain, original magnification: 20 ×. Black squares mark the regions of interest for the atomic force microscopy study. Bar = 100 μm.

With the dose increase, the negative effects of irradiation on the ECM became more evident. We studied a series of samples harvested 1 day postirradiation with the doses of 2, 8, 10, 12, and 22 Gy. Although no changes were observed at the low dose of 2 Gy, the higher doses caused a visible radiation damage in the bladder and rectum ECM, ranging from relatively minor changes at the 8 Gy dose up to severe destructive effects at the dose of 22 Gy. The signs of the ECM destruction included loosening of the network of collagen fibers and release of a great amount of nonfibrous ECM material covering the collagen fibers, as well as thickening and disordering of collagen fibrils inside the fibers. The radiation effect on the rectum appeared more pronounced than that on the bladder, with the similar changes taking place at a lower dose. At the highest studied dose of 22 Gy, the entire collagen hierarchical structure in the submucosa of the bladder and rectum underwent major changes with collagen fibers sticking together to form thick oriented bundles continuously covered with the nonfibrous matrix elements. The observed visual changes in the ECM morphology with the dose increase were well correlated with the findings of the FNS analysis. Indeed, the growth of the FNS parameters with the radiation dose reflected the growing disorder in the structure due to the destruction process, whereas the decrease of the FNS parameters at the highest dose of 22 Gy was obviously related to formation of the thick oriented bundles coated with the released unstructured ECM material such as GAG. The FNS sensitivity to the changes occurring with the increase of the radiation dose (as opposed to the lack of sensitivity in the time dependence) may be explained by the fact that all the samples were studied at the very early time after the irradiation (1 day), when the initial processes of ECM destruction dominate over all the other related processes.

The identical dose-dependent changes in the bladder and rectum observed both visually and via the FNS study were compared with the dose dependence for a different type of connective tissue—abdominal skin, to reveal whether the observed changes have a general character. Indeed, a striking similarity was found between all the three tissues—bladder, rectum, and skin—in both the results of AFM imaging study and the FNS

https://doi.org/10.1017/S1431927618000065 Published online by Cambridge University Press

parameterization, which points to the same mechanisms of the collagen matrix alteration taking place early after the irradiation.

The success of radiotherapy in eradicating a tumor depends principally on the total radiation dose given, but the tolerance of the normal tissues surrounding the tumor limits this dose. Radiation dose–response relationships for the normal tissues have a threshold at low doses (which produce no reaction) and saturate at high doses (Barnett et al., 2009). There is evidence that the normal tissue radiation dose–response relationships are steep; this means that small changes in the dose result in relatively large differences in toxicity (Turesson, 1990; Bentzen et al., 2008). In our study with the use of the FNS analysis, we have not reliably detected any jump-like changes in the collagen state of the irradiated organs with the dose increase in the range of 2–12 Gy (Fig. 8). The observed decrease of the FNS parameters at 22 Gy is more probably related to the above-mentioned reasons than to the growth of the order at the level of collagen fibers.

Although AFM imaging showed the first signs of the low-dose radiation damage of the bladder and rectum ECM already in a week after the treatment and dramatic changes 1 month post-irradiation, the parallel histological study using the standard Van Gieson's stain did not reveal any significant alterations indicating the radiation damage. In the case of the dose dependence, the AFM study along with the FNS parameterization provided more details in the description of the samples' changing morphology than the corresponding histological study. This ability of the nanoscale ECM structure (collagen fibrils) to respond early to the radiation damage has been previously shown in electron microscopy (Leontiou et al., 1993) and nanoindentation (Lindburg et al., 2013) studies. Our AFM results on the time and dose dependence of the radiation damage of bladder and rectum also appear in a good agreement with the previously obtained microscale data of second harmonics generation and multiphoton microscopy (Kochueva et al., 2014; Kuznetsov et al., 2016). Thus, the techniques for studying the collagen packing in the ECM of irradiated tissues appear more sensitive to the early radiation damage in the bladder and rectum than conventional histology methods, providing valuable additional information on the onset and development of the ECM destruction and remodeling.

Conclusions

In this study, we have tracked the early negative effects of ionizing radiation on the submucosal region of the pelvic organs—bladder and rectum, which appear the primary targets for the healthy tissue damage in the radiation therapy of pelvic tumors. Our study consisted of two parts, one of which was dedicated to the effects of low-dose (2 Gy) radiation on a time scale after the treatment (1 day, 1 week, and 1 month), whereas the other part was related to the very early (1 day postirradiation) effects of increasing radiation doses (2, 8, 10, 12, 22 Gy).

According to our AFM findings, the low-dose (2 Gy) radiation had no immediate (1 day posttreatment) effect on the collagen structures in the bladder and rectum. The first changes were observed 1 week after the radiation treatment at the level of collagen fibrils. In the bladder, we observed a release of the nonfibrous ECM material covering the fibrils and in the rectum the fibrils tended to become thicker and denser packed. No alterations were found at the level of the ECM microstructure (collagen fibers and their bundles). We assign these initial alterations in the morphology of collagen fibrils to the protein matrix destruction which is known to occur as the first stage of the radiation damage development in the ECM.

1 month postirradiation in the dose of 2 Gy, AFM imaging detected thick bundles of oriented collagen fibers with the quasi-parallel fibrils inside the fibers both in the bladder and rectum. These findings evidently indicated the onset of postradiation fibrotic changes, in accordance with the previously reported data of multiphoton and second harmonics microscopy studies.

The traditional histological study using Van Gieson picro-fuchsin stain has not found any significant changes in the ECM of the bladder and rectum, even 1 month postirradiation, thus demonstrating that AFM is a more sensitive technique in tracking the low-dose radiation damage.

Although no effect was observed 1 day after the irradiation in the low dose (2 Gy), the higher doses caused noticeable radiation damage, its severity growing proportionally with the radiation dose. The signs of the ECM destruction visualized by AFM imaging involved: loosening of the packing of collagen fibers, thickening and disordering of fibrils' assembly inside the fibers, and release of unstructured nonfibrous ECM material (such as GAG) covering the collagen backbone in a thick layer. The destructive effect of ionizing radiation appeared more severe in the rectum than that in the bladder. At the 22 Gy dose, the entire collagen hierarchical 3D network of the normal bladder and rectal ECM was restructured into the fibrotic-type collagen architecture (thick oriented bundles of fibers covered with the unstructured ECM material). The visual findings of AFM imaging on the growing degree of the ECM damage with the radiation dose correlated well with the findings of the quantitative FNS analysis of AFM images. For comparison, we also studied the dose dependence for a different type of connective tissue—abdominal skin from within the irradiated area. We found a striking similarity between the bladder, rectum, and skin both in the results of AFM imaging and in the dose dependencies of the FNS parameters, which pointed out to a generalized character of the collagen matrix alterations occurring very early after the radiation treatment.

The previous studies have shown that techniques capable of detecting changes in the collagen structure at the micron and submicron level appear superior in the detection of early radiation damage to the standard histological assessment. Our study suggests that AFM, as a high-resolution micro- and nanoscale modality, along with the FNS technique of AFM image processing, may provide new valuable information on the onset and early course of the radiation-induced damaging processes in the collagen structures of the pelvic organs subjected to radiation therapy.

Acknowledgments. This study was financially supported by the Russian Foundation for Basic Research, grant no. 15-02-04505 (AFM, clinical studies) and by the Russian Science Foundation, grant no. 16-15-10432 (preparation of samples, histological studies).

References

Atkinson MJ (2013) Radiation treatment effects on the proteome of the tumour microenvironment. In *Advances in Experimental Medicine and Biology, Volume 990: Radiation Proteomics*, Leszczynski, D (Ed.), pp. 49–60. Berlin: Springer.

Balli E, **Comelekoglu U**, **Yyalin E**, **Yilmaz N**, **Aslantas S**, **Sogut F**, **Berkoz M and Yalin S** (2009) Exposure to gamma rays induce early alterations in skin in rodents: Mechanical, biochemical and structural responses. *Ecotoxicol and Environ Saf* **72**, 889–894.

https://doi.org/10.1017/S1431927618000065 Published online by Cambridge University Press

Barnett GC, West CML, Dunning AM, Elliott RM, Coles CE, Pharoah PDP and Neil GB (2009) Normal tissue reactions to radiotherapy towards tailoring treatment dose by genotype. *Nat Rev Cancer* **9**(2), 134–142.

Bentzen SM, Agrawal R, Aird EG, Barrett JM, Barrett-Lee PJ, Bliss JM, Brown J, Dewar JA, Dobbs HJ, Haviland JS, Hoskin PJ, Hopwood P, Lawton PA, Magee BJ, Mills J, Morgan DA, Owen JR, Simmons S, Sumo G, Sydenham MA, Venables K and Yarnold JR (2008) The UK Standardisation of Breast Radiotherapy (START) trial A of radiotherapy hypofractionation for treatment of early breast cancer: A randomised trial. *Lancet Oncol* **9**, 331–341.

Choy J, Mathieu-Costello O and Kassab G (2005) The effect of fixation and histological preparation on coronary artery dimensions. *Ann Biomed Eng* **33**, 1027–1033.

Denham JW and Hauer-Jensen M (2002) The radiotherapeutic injury—a complex "wound". *Radiother Oncol* **63**, 129–145.

Dorph-Petersen KA, Nyengaard JR and Gundersen HJ (2001) Tissue shrinkage and unbiased stereological estimation of particle number and size. *J Microsc* **204**, 232–246.

Graham HK, Hodson NW, Hoyland JA, Millward-Sadler SJ, Garrod D, Scothern A, Griffiths CEM, Watson REB, Cox TR, Erler JT, Trafford AW and Sherratt MJ (2010) Tissue section AFM: In situ ultrastructural imaging of native biomolecules. *Matrix Biol* **29**, 254–260.

Grant RA, Cox RW and Kent CM (1973) The effects of gamma irradiation on the structure and reactivity of native and cross-linked collagen fibres. *J Anat* **115**, 29–43.

Jorba I, Uriarte JJ, Campillo N, Farre R and Navajas D (2017) Probing micromechanical properties of the extracellular matrix of soft tissues by atomic force microscopy. *J Cell Physiol* **232**, 19–26.

Kim T, Sridharan I, Ma Y, Zhu B, Chi N, Kobak W, Rotmensch J, Schieber JD and Wang R (2016) Identifying distinct nanoscopic features of native collagen fibrils towards early diagnosis of pelvic organ proelapse. *Nanomedicine* **12**, 667–675.

Kochueva MV, Sergeeva EA, Ignatieva NY, Zakharkina OL, Kuznetsov SS, Kiseleva EB, Babak KV, Kamensky VA and Maslennikova AV (2014) The study of radiation-induced damage and remodeling of extracellular matrix of rectum and bladder by second-harmonic generation microscopy. *Proc SPIE* **8948**, 894809.

Kotova SL, Timashev PS, Guller AE, Shekhter AB, Misurkin PI, Bagratashvili VN and Solovieva AB (2015) Collagen Structure deterioration in the skin of patients with pelvic organ proelapse determined by atomic force microscopy. *Microsc Microanal* **21**, 324–333.

Kuznetsov SS, Dudenkova VV, Kochueva MV, Kiseleva EB, Ignayieva NY, Zakharkina OL, Sergeeva EA, Babak KV and Maslennikova AV (2016) Multiphoton microscopy in the study of morphological characteristics of radiation-induced injuries of the bladder. *Sovrem Technol Med* **8**, 31–39.

Kwok J, Grogan S, Meckes B, Arce F, Lal R and D'Lima D (2014) Atomic force microscopy reveals age-dependent changes in nanomechanical properties of the extracellular matrix of native human menisci: Implications for joint degeneration and osteoarthritis. *Nanomedicine* **10**, 1777–1785.

Leontiou I, Matthopoulos DP, Tzaphlidou M and Glaros D (1993) The effect of gamma-irradiation on collagen fibril structure. *Micron* **24**, 13–16.

Lindburg CA, Willey JS and Dean D (2013) Effects of low dose X-ray irradiation on porcine articular cartilage explants. *J Orthop Res* **31**, 1780–1785.

Maslennikova A, Kochueva M, Ignatieva N, Vitkin A, Zakharkina O, Kamensky V, Sergeeva E, Kiseleva E and Bagratashvili V (2015) Effects of gamma irradiation on collagen damage and remodeling. *Int J Radiat Biol* **91**, 240–247.

Maver U, Velnar T, Gaberscek M, Planinsek O and Finsgar M (2016) Recent progressive use of atomic force microscopy in biomedical applications. *Trends Analyt Chem* **80**, 96–111.

Mirsaidov U, Timashev SF, Polyakov YUS, Misurkin PI, Musaev I and Polyakov SV (2011) Analytical method for parameterizing the random profile components of nanosurfaces imaged by atomic force microscopy. *Analyst* **136**, 570–576.

National Institutes of Health (2010) *Common Terminology Criteria for Adverse Events, Version 4.0*. Bethesda, MD: Cancer Therapy Evaluation Program, National Cancer Institute, National Institutes of Health.

Reisz JA, Bansal N, Qian J, Zhao W and Furdui CM (2014) Effects of ionizing radiation on biological molecules—mechanisms of damage and emerging methods of detection. *Antioxid Redox Signal* **21**, 260–292.

Sivasankar M and Ivanisevic A (2007) Atomic force microscopy investigation of vocal fold collagen. *Laryngoscope* **117**, 1876–1881.

Stolz M, Gottardi R, Raiteri R, Miot S, Martin I, Imer R, Staufer U, Raducanu A, Duggelin M, Baschong W, Daniels AU, Friederich NF, Aszodi A and Aebi U (2009) Early detection of aging cartilage and osteoarthritis in mice and patient samples using atomic force microscopy. *Nat Nanotechnol* **4**, 186–192.

Thomasy SM, Raghunathan VK, Winkler M, Reilly CM, Sadeli AR, Russell P, Jester JV and Murphy CJ (2014) Elastic modulus and collagen organization of the rabbit cornea: Epithelium to endothelium. *Acta Biomaterialia* **10**, 785–791.

Timashev PS, Kotova SL, Belkova GV, Gubar'kova EV, Timofeeva LB, Gladkova ND and Solovieva AB (2016) Atomic force microscopy study of atherosclerosis progression in arterial walls. *Microsc Microanal* **22**, 311–325.

Trott K-R, Doerr W, Facoetti A, Hopewell J, Langendijk J, van Luijk P, Ottolenghi A and Smyth V (2012) Biological mechanisms of normal tissue damage: Importance for the design of NTCP models. *Radiother Oncol* **105**, 79–85.

Turesson I (1990) Individual variation and dose dependency in the progression rate of skin telangiectasia. *Int J Radiat Oncol Biol Phys* **19**, 1569–1574.

Tzaphlidou M, Kounadi E, Leontiou I, Matthopoulos DP and Glaros D (1997) Influence of low doses of gamma-irradiation on mouse skin collagen fibrils. *Int J Radiat Biol* **71**, 109–115.

Wallace JM (2012) Applications of atomic force microscopy for the assessment of nanoscale morphological and mechanical properties of bone. *Bone* **50**, 420–427.

Wen C-Y, Wu C-B, Tang B, Wang T, Yan C-H, Lu WW, Pan H, Hu Y and Chiu K-Y (2012) Collagen fibril stiffening in osteoarthritic cartilage of human beings revealed by atomic force microscopy. *Osteoarthritis Cartilage* **20**, 916–922.

Yarnold J and Brotons MCV (2010) Pathogenetic mechanisms in radiation fibrosis. *Radiother Oncol* **97**, 149–161.

Zhu P and Fang M (2012) Nano-morphology of cartilage in hydrated and dehydrated conditions revealed by atomic force microscopy. *J Phys Chem Biophys* **2**, 1–3.

https://doi.org/10.1017/S1431927618000065 Published online by Cambridge University Press